



## Studying of contact electrification and electron transfer at liquid-liquid interface

Xiuzhong Zhao<sup>a,b</sup>, Xiao Lu<sup>a</sup>, Qiwei Zheng<sup>a,b</sup>, Lin Fang<sup>a,b</sup>, Li Zheng<sup>a,\*</sup>, Xiangyu Chen<sup>b,\*</sup>, Zhong Lin Wang<sup>b,c,\*\*</sup>

<sup>a</sup> College of Mathematics and Physics, Shanghai Key Laboratory of Materials Protection and Advanced Materials in Electric Power, Shanghai University of Electric Power, Shanghai 200090, PR China

<sup>b</sup> CAS Center for Excellence in Nanoscience, Beijing Key Laboratory of Micro-nano Energy and Sensor, Beijing Institute of Nanoenergy and Nanosystems, Chinese Academy of Sciences, Beijing 100083, PR China

<sup>c</sup> School of Materials Science and Engineering, Georgia Institute of Technology, Atlanta, GA 30332, USA

### ARTICLE INFO

#### Keywords:

Triboelectric nanogenerator  
Liquid-liquid contact electrification  
Electrostatic shielding effect  
Ion transfer  
Electron transfer

### ABSTRACT

Triboelectric nanogenerator (TENG) provides an effective approach for studying transferred charges at solid-solid or liquid-solid interfaces. Here, by dripping a liquid droplet through an immiscible organic solution (transformer oil), we used single-electrode mode TENG to measure the transferred charges on the liquid droplet once it goes down in the solution. The falling droplets (with volume of 25  $\mu\text{L}$ ) can generate negative charges on its surface and the output charges amount can reach  $-5.3\text{pC}$  by passing through the transformer oil. In addition, we found that both the pH value and the electrostatic shielding effect of free ions greatly hinder the electron transfer efficiency at L-L contact electrification. Combining the experimental results and previous research, we infer that there are both ion transfer and electron transfer happening in the L-L electrification.

### 1. Introduction

Since triboelectric nanogenerator (TENG) was proposed by Wang et al. in 2012, it has gradually become a hot research field because of its cost-efficient energy collection capacity [1–4]. The working principle of TENG is based on the coupling effect of contact electrification and electrostatic induction. The displacement current of Maxwell equation caused by relative displacement of different contact surfaces due to the action of external mechanical force is the main reason for the output of external current. Based on the coupling effect of contact electrification (CE) and electrostatic induction, TENG is a novel technology used to collect micro-nano energies in the natural environment. So far, due to the universality of contact electrification, TENGs can harvest many kinds of mechanical energy generated by CE between various material interfaces, including solid-solid (S-S) interface [5–10], solid-liquid (S-L) interface [11–13], and even liquid-liquid (L-L)/gas(G) interface [14–16]. After continuous development, S-S and S-L TENG has shown excellent performance in the area of micro-nano energy harvesting, human-computer interaction, sensor, pollutant cleaning and so on [6–8,

17–19]. Although a large amount of development has been carried out based on TENG and related applications, there are few related researches on energy harvesting of the L-L interface in contrast to S-S TENG and S-L TENG [20–29], the working mechanism of L-L TENG is still not fully revealed. Meanwhile, due to ion adsorption and molecular thermal motions [30–33], it is quite difficult to achieve complete separation between two liquids and thus, more efforts should be devoted to the study of the energy collection on L-L interface.

In order to achieve effective separation at the L-L interface, Chen et al. developed a highly durable liquid membrane to collect energy from liquid droplets, and Wang et al. applied super-lubricating interface to realize energy harvesting from L-L interface [14,15]. Recently, Wang et al. also successfully realized triboelectric charge collection between liquid and liquid by using the super affinity of lubricant oil and PTFE membrane. However, in their experiments, the thickness of the liquid interface is only 2  $\mu\text{m}$ , which is difficult to completely avoid the influence of the PTFE film during L-L CE [15]. In addition, Jiang et al. successfully detected the charge signal at the oil/water interface by using single-electrode L-S TENG [16], but they did not quantify the L-L CE

\* Corresponding authors.

\*\* Corresponding author at: CAS Center for Excellence in Nanoscience, Beijing Key Laboratory of Micro-nano Energy and Sensor, Beijing Institute of Nanoenergy and Nanosystems, Chinese Academy of Sciences, Beijing 100083, PR China.

E-mail addresses: [zhengli@shiep.edu.cn](mailto:zhengli@shiep.edu.cn) (L. Zheng), [chenxiangyu@binn.cas.cn](mailto:chenxiangyu@binn.cas.cn) (X. Chen), [zlwang@gatech.edu](mailto:zlwang@gatech.edu) (Z.L. Wang).

<https://doi.org/10.1016/j.nanoen.2021.106191>

Received 23 March 2021; Received in revised form 20 May 2021; Accepted 21 May 2021

Available online 26 May 2021

2211-2855/© 2021 Published by Elsevier Ltd.

charge and study the influence factors.

Here, we designed an experimental system with strong immunity to environmental electromagnetic interference, which can help to clarify the electrification process between liquid droplets and transformer oil. In this system, deionized (DI) water droplets are dripped freely and continuously into transformer oil, while a TENG with single electrode mode is placed at the bottom of oil. Thus, a complete L-L CE energy collection system is realized. Based on this system, we have clarified several important issues. Firstly, during the droplet falling, the charges on the surface of the droplet can gradually accumulate and output charge of  $-5.3\text{pC}$  can be obtained from our L-L TENG. Secondly, the key parameter for this electrification is the relative falling speed of droplet, which can decide the separation process between droplet and the surrounding transformer oil. Meanwhile, due to the internal circulation of transformer oil, the total amount of transferred charges on the droplet surface finally reaches saturation. In addition, we also studied the influence of solute and pH value on L-L CE, and the results show that there is also electrostatic shielding phenomenon, where  $\text{OH}^-$  or  $\text{H}^+$  ions play an important role in L-L CE. Finally, based on experimental measurement and theoretical derivation, the charge transfer mechanism of the L-L interface and a simple electric double layer (EDL) model are proposed.

## 2. Results and discussions

### 2.1. The structure of L-L triboelectric nanogenerator

Fig. 1a shows a dynamic CE process between DI water droplets and transformer oil (25#). To keep the DI water droplets' sliding channel in oil remaining stable, an adjustable high-precision stepper motor is used to push DI water droplets into the oil at a steady speed. At the same time, with the protection of electrostatic shielding of the Faraday cage, all environmental noise interference from outside is greatly reduced in the process of CE, with noise signal of only a few pA when the system is in stable state. The photograph of this experimental apparatus is shown in Fig. S1. Furthermore, in order to reduce the effects of material and shape of the container on the internal circulation of the transformer oil, a big cylindrical dish made of crystallized glass is used as the container for transformer oil. In addition, a needle-shaped copper electrode is placed near the bottom of the oil, and the output electrical signal of L-L CE can be exported through a shielded wire connected with the copper electrode. Due to the small size of needle-shaped copper electrode and the shielded wire, the internal movement of the transformer oil can be hardly affected. The low molecular weight of transformer oil and its immiscibility with water make it easy to repeat CE progress in liquid

phase, while the insulation characteristics of transformer oil allows us to directly connect the external shielded wire to the transformer oil to measure the output signal of water-oil contact electrification. Relying on the gravity (the molecular weight of transformer oil is 0.895), the CE between falling DI water droplets and transformer oil proceeds autonomously without any interference from other charged objects. Specifically, the CE process is started and tested fully inside the oil, which is quite different from previous L-L TENGs' method for harvesting mechanical energy [5–10]. Hence, the charges on liquid droplets' surface generated by CE between transformer oil and DI water can be clearly analyzed based on this system.

The stability of the droplets' sliding channel (i.e. CE channel in the oil liquid) is a critical factor for systematical study on the influence of contact area, displacement distance, solute and liquid temperature on L-L CE process. To control the stability of the electrification process between liquid droplets and transformer oil, we use a liquid droplet squeezing method for this experiment, as shown in Supporting Fig. S1. A grounded needle that serves as the electrode for TENG is fixed on a vertical linear motor, and the distance between liquid droplets and transformer oil surface can be precisely controlled by a lifting platform and all liquid droplets will slide off at a fixed height into the transformer oil surface. As liquid droplets continuously fall at a certain speed, a symmetrical circulation happens in the transformer oil solution near the droplet sliding channel (Fig. 1b and Supporting Video 1). Fig. 1b illustrates a set of photographs showing the dynamic internal circulation process of the transformer oil. Here, the driving force for the formation of internal circulation comes from the frictional force (or viscous force) between falling liquid droplets and the transformer oil solution. Accordingly, the relative speed between droplet and surrounding oil is the key parameter. Obviously, when the relative velocity is infinitely close to 0, the frictional motion between droplet and transformer oil cannot happen. Therefore, by controlling the sliding velocity of the droplets, the relative displacement distance between the liquid-liquid interface can be effectively controlled. In the process of internal circulation, the speed of internal circulation is gradually reduced along with the radial direction from the sliding channel, and the pristine transformer oil in position far enough hardly participate. Thus, the influence of the container on the electrification process is further excluded. Due to the obvious speed difference between DI water droplets and transformer oil surrounding the sliding channel, all DI water droplets continuously contact with pristine transformer oil during falling process, and the oil that has been in contact with DI water droplets continues to be left behind. According to previous research [30–32], DI water droplets are negatively charged when oil and water are in contact, which is

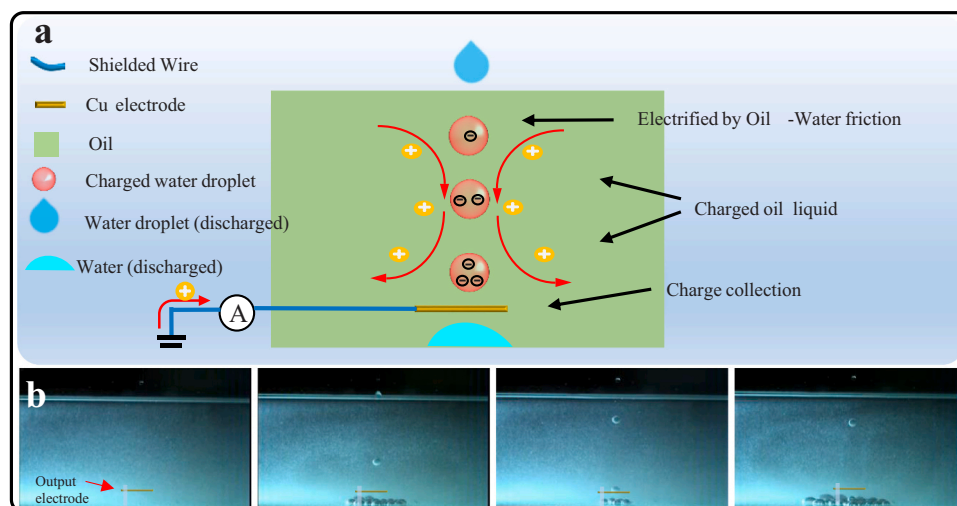


Fig. 1. a) The dynamic liquid-liquid contact electrification process and experimental method for measuring the amounts of charges on the DI water droplet. b) A set of photographs showing the internal circulation process of falling droplets.

consistent with our experimental results. As L-L CE process continues, charges on liquid droplet' surface reach a maximum at a certain position during the sliding process. When a liquid droplet touch with the copper electrode, the amounts of charges on the liquid droplet' surface can be extracted to the external circuit and be measured with Keithley 6517B. Although fresh uncontacted oil solution is constantly added to the internal circulation, due to the law of charge conservation, the charges of the droplet' surface will reach a saturation state when enough L-L CEs occur. Hence, the stability of liquid droplets' sliding channel and the saturation state of triboelectricity may be key factors to study the mechanism of L-L CE. In our research, the same experiment was redone by employing dozens of fresh transformer oil, and only the charges generated from the first three contacted transformer oil was recorded for data analysis.

Supplementary material related to this article can be found online at [doi:10.1016/j.nanoen.2021.106191](https://doi.org/10.1016/j.nanoen.2021.106191).

## 2.2. Electrical output of L-L CE

To study the mechanism of CE between DI water droplets and transformer oil, the amounts of charges contained in droplets falling from different heights after contacting with transformer oil is measured, as shown in the Fig. 2, and the corresponding output current is shown in Supporting Fig. S2. As shown in the Figs. 2 and S2, the amounts of output charges can reach about  $-5.3\text{pC}$  under a very short friction distance. In this set of experiments, the volume of all DI water droplets is kept to be  $25\ \mu\text{L}$  and released from heights (Defined as  $h$ ) of 0 mm, 10 mm and 20 mm from the oil surface, respectively. Through force analysis, according to Newton's second law and the velocity formula, the velocity of the liquid droplet is calculated as  $V \cong 0, 0.445, 0.629, 0.770\ \text{m/s}$ .

As introduced above, falling droplets of different heights have significantly different velocity when they reach oil surface. Fig. S3 shows a series of photographs illustrating that the fluctuations caused by droplets from different falling heights are significantly different, and the fluctuations become more obvious as falling velocity increases. The related current output of one droplet induced on TENG electrode is shown in Fig. 2a. When the falling height  $h = 0\ \text{mm}$ , there is almost no fluctuation when the droplet passes through the oil surface. However, when the falling height reach 30 mm, the droplet will deform and split significantly due to the excessive momentum of the droplet. Therefore, the highest position of the droplets falling is about 20 mm in this experiment. During the sliding, the CE between DI water droplet and

transformer oil leads to charge accumulation on the droplet surface.

In many cases, water usually loses electrons when it contacts with other objects. However, in Fig. 2a we can clearly see that the DI water droplets that have been in contact with transformer oil carry negative charges, which is a phenomenon worth discussing regarding the mechanism of CE in L-L. Meanwhile, the contact and separation of water droplet with Cu electrode leads to an alternative current signal, which characterize the charges transferred once the droplet contacts the electrode and leave the electrode. Fig. S4 shows the transfer process of charges between droplet and electrode. The transformer oil around the electrode has a very small amounts of negative charges because Cu usually loses electrons (Fig. S4a). The droplets continuously accumulate large amounts of negative charges in falling progress (Fig. S4b) and when the droplet contacts with the electrode, these negative charges are transferred to external circuit through the needle electrode. Hence, as can be seen in Fig. 2a, the negative current signal is stronger than the positive one. At the same time, when the droplet contacts with the electrode, the negative charges attached to the electrode move around due to motion of oil liquid (Fig. S4c). After the droplet separates from the electrode, the transformer oil reassembles around the electrode and results in another current signal (Fig. S4d). The charge exchange between droplet and electrode causes unbalance between the positive and negative current peaks. Therefore, the difference between the positive and negative peaks is the output current on the surface of the droplet. From the data comparison in Fig. 2a, we can clearly see that the output current increases with the increase of falling height. And the increase of output current is uniform when the drop height  $h$  is 0 mm, 10 mm, 20 mm. As can be seen from the inset in Fig. 2a, the fluctuations caused by falling droplets of different falling heights have a significant impact on the output current. In order to clarify the increasing effect of different speeds on the output current, we record the output current of 5 cycles to obtain the value of both positive and negative charges, as shown in Fig. 2b, c, d, respectively. The difference between positive and the negative charge is assumed to be the output charge carried by the droplet. Here, the positive charge is defined as  $Q_1$ , and the negative charge is defined as  $Q_2$ , while the output charge from the droplet to the electrode is  $\Delta Q = |Q_1| - |Q_2|$ . It is important to note that the output charge is proportional to the charge induced by L-L CE on the droplet, while it may also be influenced by the original charges carried on the droplet. As the falling height increases, the output charges accumulated on the surface of DI water droplets increases.

In fluid mechanics, the viscous resistance  $f \propto v$  of the spherical object

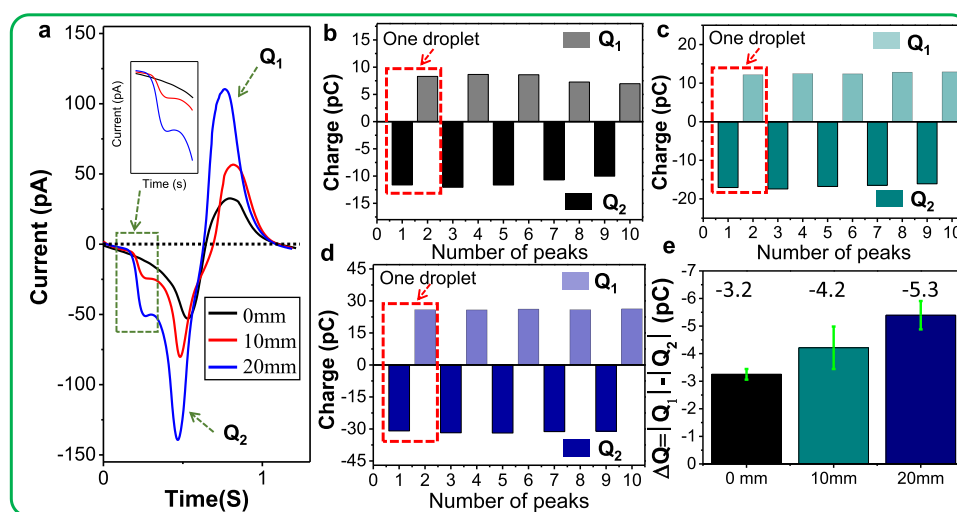


Fig. 2. a). A magnified periodic output current curve caused by droplets falling at different heights. Charges on droplet surface falling at different heights (b. 0 mm. c. 10 mm. d. 20 mm.) e). The average value of the  $\Delta Q$  caused by droplets falling at different heights ( $\Delta Q = |Q_1| - |Q_2|$  is the difference between positive charge( $Q_1$ ) and the negative charge( $Q_2$ ) and is defined as the output charge).

moving in the liquid. The faster the speed, the greater the viscous force between the liquid droplets and the transformer oil, resulting in a faster replenishment of the uncontacted transformer oil near the sliding channel. Therefore, the faster the droplet velocity, the later the attenuation of the output current at the initial stage will appear. Under the combined action of viscous resistance, buoyancy and gravity, the velocity of the droplet in the transformer oil eventually reached a stable value. Therefore, the relative displacement between the droplet and the transformer oil interface fundamentally depends on the deceleration process of the droplet in the transformer oil. In this group of experiments, the average value of the  $\Delta Q$  in the first 5 cycles is compared, as shown in Fig. 2e. It can be clearly seen that the amounts of  $\Delta Q$  rapidly increase with the increase of sliding speed (the initial speed of the droplets entering the water increases).

### 2.3. Saturation effects of the L-L CE

As the droplets' falling height increases, the impact of liquid surface fluctuations on the output current is more obvious, which can be seen in Figs. 2a and S2. In order to eliminate the fluctuation of the liquid surface and the influence of air on the charges of the droplet itself, the falling height  $h$  of all droplets in the following experiment is set to be 0 mm. We increase the droplet falling frequency from about 1 time/s to 1.7 times/s to ensure that the internal circulation of the transformer oil can occur continuously. At the same time, we increased the circulation times of DI water droplets, and obtained the changing trend of output current from water-oil contact electrification, as shown in Fig. 3a. As circulation times of falling DI water droplets increases, the output current gradually decreases. When the amounts of output charges reach a saturated state, the output current tends to stabilize. In Fig. 3a, we can clearly see that after 290 s, the output current continues to attenuate and finally reaches a saturated state. The actual process of contact electrification between transformer oil and DI water droplets is the stage where the output current gradually decreases, which we define as the actual triboelectrification. In order to better study the changing trend of the amounts of output charges, we use Origin to integrate the positive and

the negative output current of every droplet, as shown in Fig. 3b. Simultaneously fit the difference between positive charge ( $Q_1$ ) and negative charge ( $Q_2$ ), as shown in Fig. 3c. It can be seen from the fitting result that as the times of CE increases, the decay rate of the output charges ( $\Delta Q$ ) gradually slows down, which is similar to a negative exponential function curve. From Supporting Video 1, we believe that the reason for this phenomenon is that during the internal circulation of oil solution, the circulation speed of the transformer oil near the sliding channel at the initial stage is slow, thus the replenishment speed of new transformer oil around it is slow. At the middle stage, the circulation speed increases, and the replenishment speed of brand-new oil also increases, but the proportion of the contacted oil that has been contacted near the circulation sliding channel is still high. At this time, the total amount of available charge positions in the mixed oil solution near the sliding channel is still lower than the initial stage, so the decay rate of the output charge is reduced, and the total amount of available charge positions is still lower than the initial stage. For the final stage, as the times of CE increases, all the oil solution in the internal circulation area is contacted, and the available charge positions of the transformer oil solution in the internal circulation area are completely filled. At this time, the output charge transfer between DI water droplet surface and transformer oil maintain equilibrium and enters saturation. It is worth noting that because the L-L CE only has a small amount of electricity and is quite easily affected by small disturbance, the output current and saturation current of each set of experiments are unstable. However, the output charge quantity after data processing is relatively stable, so the change of the output charge quantity can accurately reflect the changing trend.

Furthermore, in order to further analyze the dominating parameters for this system, we change the volume of DI water droplets. As shown in Fig. S5, by adjusting the size of the needle tube to obtain droplets in different volumes. Here, we use DI water droplets of 60  $\mu\text{L}$ , 35  $\mu\text{L}$ , 25  $\mu\text{L}$ , and the corresponding surface areas are 0.74  $\text{cm}^2$ , 0.52  $\text{cm}^2$ , and 0.41  $\text{cm}^2$ , respectively. In this group of experiments, the depth of the transformer oil solution is kept as 40 mm. Through enough cycles of CE, the integral and fitting results of the output current of CE between oil

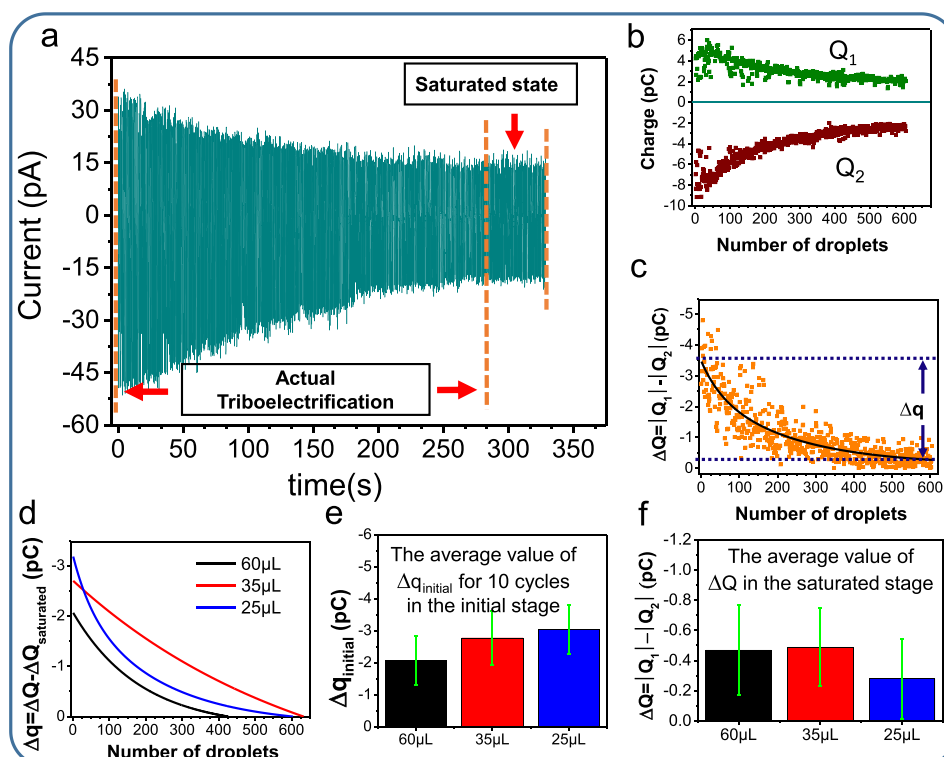


Fig. 3. a). Output current of CE between liquid droplets and oil solution over time. b). The integral result of positive charge ( $Q_1$ ) and negative charges ( $Q_2$ ) c). Fitting curve of  $\Delta Q$  and  $\Delta q$  d). Comparison the fitting curves of  $\Delta q$  with different volumes. e). The average value of  $\Delta q_{\text{initial}}$  for 10 cycles in the initial stage. ( $\Delta q = \Delta Q - \Delta Q_{\text{saturated}}$  is the transferred charges from the oil to droplet and  $\Delta q_{\text{initial}} = \Delta Q_{\text{initial}} - \Delta Q_{\text{saturated}}$  is the  $\Delta q$  in the initial stage.  $Q_{\text{initial}}$  is the  $\Delta Q$  in the initial stage,  $\Delta Q_{\text{saturated}}$  is the  $\Delta Q$  in the saturated stage), f). The average value of  $\Delta Q$  for 10 cycles in the saturated stage. ( $\Delta Q = |Q_1| - |Q_2|$  is the difference between positive charge ( $Q_1$ ) and the negative charge ( $Q_2$ )).

and water droplets in different volume can be obtained showed in Fig. S6. As we explained in Fig. 2, in order to calculate the actual charges on the droplet induced by L-L CE, we need remove the original charges on the droplet. Here, we define a parameter of transferred charges from the oil to droplet ( $\Delta q$ ), which is the difference between the output charge and  $\Delta Q$  in saturated state ( $\Delta Q_{\text{saturated}}$ ). Therefore, the transferred charge  $\Delta q = \Delta Q - \Delta Q_{\text{saturated}}$  is shown in Fig. 3c. By comparing the change trend of  $q$ , the charge interference from the syringe and the needle can be avoided. According to the same data processing method in Fig. 3a–c, the fitting curve of transferred charges from the oil to droplet ( $\Delta q$ ) for different contact areas is shown in Fig. 3d. As the contact area increases, the amounts of transferred charges accumulated on DI water droplet surface decrease accordingly. The transferred charges accumulated on the surface of 60  $\mu\text{L}$  droplet only reach a peak value of about  $-2.1\text{pC}$ , and decays faster than that of 35  $\mu\text{L}$  and 25  $\mu\text{L}$  droplet. The reason is that the larger contact area leads to an increase in the viscous force between the droplet and the transformer oil, which increases the internal circulation speed of the transformer oil and thus reduces the relative friction distance between the droplet and the transformer oil. Fig. 3e shows the average value for 10 cycles of the transferred charges ( $\Delta q$ ) at the initial stage, which is defined as ( $\Delta q_{\text{initial}} = \Delta Q_{\text{initial}} - \Delta Q_{\text{saturated}}$ ), where the  $\Delta Q_{\text{initial}}$  is the  $\Delta Q$  at the initial stage and the  $\Delta Q_{\text{saturated}}$  is the  $\Delta Q$  at saturated stage. Fig. 3f illustrates the output charge at saturated stage ( $\Delta Q_{\text{saturated}}$ ). As the contact area decreases, the transferred charges at initial stage ( $\Delta q_{\text{initial}}$ ) increase but the  $\Delta Q_{\text{saturated}}$  at saturated stage decrease. Hence, in this experiment, a small contact area is beneficial to increase the amounts of the transferred charges and reduce interference. It should be noted that large droplet also causes slight fluctuation in the transformer oil surface as a result of gravity, but it has no effect on the total amount of transferred charges. Finally, 25  $\mu\text{L}$  is the most ideal droplet volume for this experiment.

#### 2.4. Effects of solutes, liquid pH value and temperature on the L-L CE

In order to further explore the influence of ions concentration on the CE of L-L interface, the transferred charge between transformer oil and different aqueous solutions such as NaCl, HCl and NaOH is studied. Using the same experimental steps as study the contact area, the integral and fitting results of the output current is measured as shown in Fig. S7, and the fitting result of transferred charges ( $\Delta q$ ) on different solution droplet is shown in Fig. 4a, b (the measurement method is shown in Fig. 1a, and the data processing method is same as Fig. 3a–c.) First of all, the droplet volume of all experiments is kept at 25  $\mu\text{L}$ , and falling height  $h = 0$  mm. Fig. 4a shows the transferred charges on the surface of NaCl

droplets in different concentrations after contacting with transformer oil. When the concentration of NaCl solution is 0.001 M, the amounts of transferred charges is slightly higher than that on the surface of DI water droplets. However, when the concentration of NaCl solution is 1 M, the amounts of transferred charges decrease obviously. The comparison of the transferred charges on the droplet surface of 0.001 M and 1 M NaCl solution and DI water for 10 cycles in the initial stage is shown in Fig. 4d. When the concentration of NaCl solution is 0.001 M, the transferred charges on the droplet surface are the maximum, while when the concentration of NaCl solution increases to 1 M, the transferred charges on the surface of NaCl droplet decreases obviously. Fig. 4b separately exhibits the changing trend of the transferred charges of 0.001 M HCl and NaOH solution after contacting with transformer oil, and the comparison of transferred charges on the surface of the droplet for 10 cycles in the initial stage is shown in Fig. 4e. It can be seen that the transferred charges decrease obviously with the increase of the concentration of HCl and NaOH in the droplets. If we consider the Wang's transition model with both electrons transfer and ion absorption effect on the L-L interface, the increase of ion concentration may suppress the electron transfer on the L-L interface, which is due to the electrostatic shielding of high concentration of free ions. These results are in good agreements with Wang's model. It is also very interesting to find that the transferred charges slightly increase with NaCl solution of 0.001 M. We have found the similar effect in L-S electrification. Here, the slight increase of the transferred charges in NaCl solution of 0.001 M is possibly due to the enhancement of ion transfer process, which means the absorption of  $\text{Na}^+$  ion is possible on this L-L interface. However, the similar absorption effect is not observed in NaOH solution, which should be attributed to the interference of high mobility  $\text{OH}^-$  ion. At the same time, when the concentration of the NaCl solution reaches 1 M, the electrostatic shielding effect of the high concentration of free ions inhibits the electron transfer process between the liquid-liquid interface, resulting in a decrease in the amount of transferred charge.

Compared with solids, the distance between liquid molecules is larger, the effect of temperature on the thermal motion of liquid molecules is more obvious, and the integral and fitting result of the output current by L-L CE is shown in Supporting Fig. S8. Fig. 4c shows the variation trend of transferred charges on droplet surface at different temperatures. It is worth noting that the transformer oil used here is not the same batch in previous experiment. Therefore, this group of experimental data can't be quantitatively compared with previous one, only within this group. In Fig. 4c, it is shown that when the transformer oil and droplets are at 300 K, the number of transferred charges on the droplet surface is about  $-1.7\text{pC}$ . However, when the transformer oil and

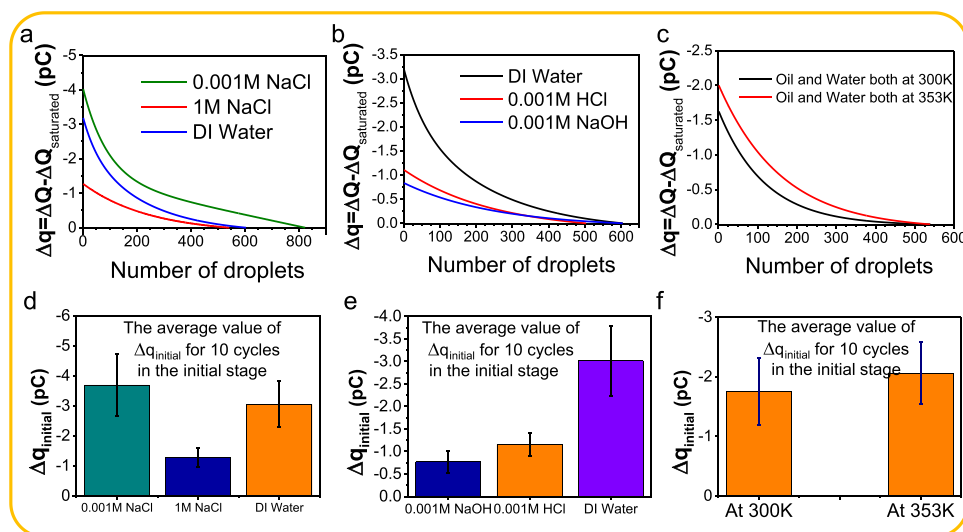


**Fig. 4.** a). Fitting curve of  $\Delta q$  in DI water, NaCl solution with solution of 0.001 M and 1 M respectively. b). Fitting curve of  $\Delta q$  of NaOH and HCl with droplet solution of 0.001 M, respectively. c). Fitting curve of  $\Delta q$  at different temperatures (the droplet volume is 25  $\mu\text{L}$ ). d, e, f). The average value of  $\Delta q_{\text{initial}}$  for 10 cycles at different ion concentration and temperature (the droplet volume is 25  $\mu\text{L}$ ). ( $\Delta Q$  is the difference between positive charge ( $Q_1$ ) and the negative charge ( $Q_2$ ),  $\Delta Q_{\text{initial}}$  is the  $\Delta Q$  in the initial stage,  $\Delta Q_{\text{saturated}}$  is the  $\Delta Q$  in the saturated stage,  $\Delta q = \Delta Q - \Delta Q_{\text{saturated}}$  is the transferred charges from the oil to droplet and  $\Delta q_{\text{initial}} = \Delta Q_{\text{initial}} - \Delta Q_{\text{saturated}}$  is the  $\Delta q$  in the initial stage.)

droplets are both at 353 K, the number of transferred charges on droplet surface increases to  $-2\text{pC}$ . The main reason for this increase is that the high temperature increases the energy of surface electrons, which causes electrons more prone to transition. Compared with the average of transferred charges for 10 cycles at the initial stage (Fig. 4f), the temperature change of 50 K exacerbated electrons transfer efficiency at water/oil interface.

According to the results, the L-L CE can be affected by the pH value of the aqueous solution, the solute in the aqueous solution and the temperature. The transformer oil used in our experiment is organic mineral oil and does not contain any free ions. Combining the experimental results and the "Wang transition" model, we propose a new model of L-L CE and electric double layer (EDL) as shown in Fig. 5a. In the first step, the droplets are in contact with the original transformer oil (see Fig. 5b–d). The molecules and ions in the two liquid phases collide with the oil-water interface due to thermal motion and the pressure of the surrounding liquid (Fig. 5b). During the impact, both electron transitions and ions reactions may occur on the transformer oil surface (Fig. 5c). Hence, there are both electrons and ions generated on the transformer oil surface. Meanwhile, based on the results of pH testing, we believe that electron transfer effect is much stronger than the adsorption of  $\text{H}^+$  on the oil/water interface. In the second step, the potential near the interface attracts some negative ions in the aqueous solution to migrate toward the interface by electrostatic interactions, thereby forming an EDL at the interface (Fig. 5d). Furthermore, the electrons that transition from the transformer oil molecules to the water molecules may not be maintained at the interface, and the electrons combine with the water molecules to form the hydrated electrons. Usually, the hydrated electrons are extremely unstable and they may turn into  $\text{OH}^-$  and  $\text{H}$  (hydrogen radical) in a very short time [34,35], leading to the high concentration of  $\text{OH}^-$  ions near the L-L interface.

### 3. Conclusion

In summary, we have established an L-L TENG by passing a liquid droplet through an immiscible organic solution. Utilizing the effect of gravity and the difference in molecular mass, the liquid droplet can

'move freely' without the influence of external force, and a complete L-L CE energy collection system is realized. The falling droplets (25  $\mu\text{L}$ ) can generate a max output charge of  $-5.3\text{pC}$  by passing through the immiscible organic liquid of 40 mm and the water molecule is able to capture electrons from oil molecule. In addition, the internal circulation of oil is formed under the continuous impact of droplets falling as a result of the existence of viscous force. The relative displacement between droplet and surrounding oil is the key parameter for generating transferred charges and we can change this relative displacement distance by adjusting initial velocity of entering DI water droplets. With continuous falling of the droplets, the amounts of transferred charges on droplet surface gradually attenuates and finally reaches a saturated state. The "Wang transition" model is employed to explain this L-L CE effect. By increasing  $\text{H}^+$  ions in the droplet, the transferred charges of L-L interface are decreased significantly, suggesting that the electron transfer may be the dominating effect on the CE interface. In addition, with the increase of temperature, the accumulated transferred charges at L-L interface increases, which is quite different from the cases of solid-solid electrification. The main reason for this phenomenon is attributed to the viscosity decrease caused by the high temperature. Finally, combining experimental results and "two-step" theory, we predict the EDL model of the L-L interface. This study reports several basic mechanism related to the L-L electrification and many interesting phenomena, including the pH value effect and temperature effect, have been clarified. The physical analysis and the experimental methods proposed here can serve as the knowledge backup for the study of pure L-L TENG.

## 4. Experimental section

### 4.1. Sample preparation

Deionized water (HHitech, China) and 25# transformer oil (TOMA, China) were selected as target targets. The density of 25# transformer oil is  $0.895\text{ g/cm}^3$ , which is the basis for the realization of autonomous friction movement. The flash point can reach more than 410k, so that the oil can maintain stable properties at 353 K.

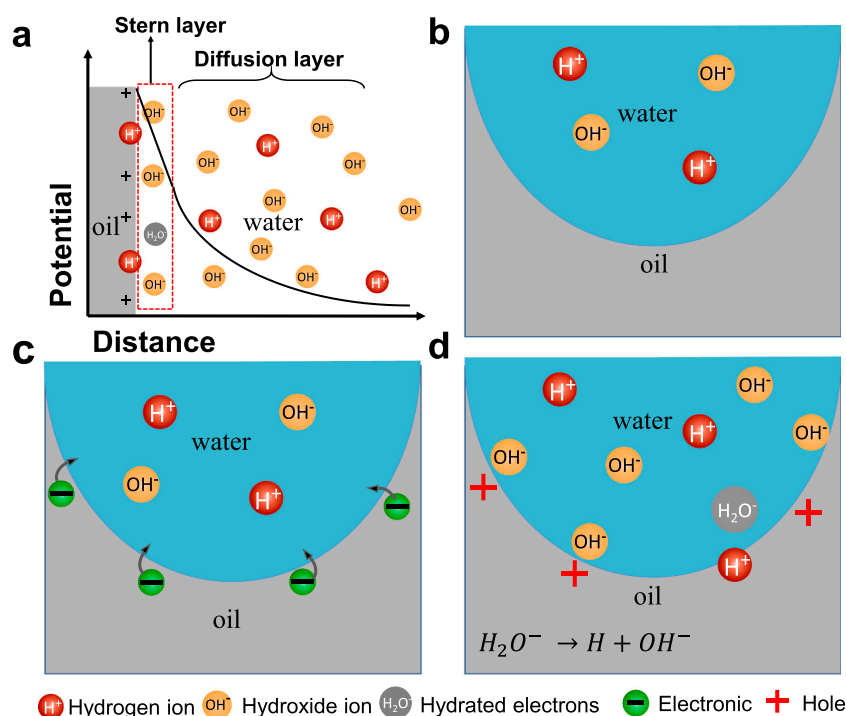


Fig. 5. a). The structure model of oil-water interface EDL. b, c, d). Charge transfer process at the L-L interface and the formation of EDL.

#### 4.2. Measurements of the surface potential of liquid droplets

A linear motor was used to drive the needle to squeeze the liquid and then the liquid droplets move autonomously through the transformer oil (Supporting Fig. 1). The linear motor controlled a squeezing velocity of  $8 \text{ mm/s}^{-1} \sim 16 \text{ mm/s}^{-1}$  and there was no dwell time in contact with the Cu electrode. Therefore, the contact time of the liquid droplet with electrode was within 0.1 s. Transformer oil was placed in a square metal shielding cage to minimize electromagnetic interference (Supporting Fig. 1). And the Cu electrode is connected by a shielded wire with Keithley 6517B. The magnitude of current can reach as high as  $60 \mu\text{A}$ . Due to the insufficient accuracy of Keithley 6517B, the transfer charge on the surface of droplet needs to be calculated using Origin for integral calculation.

#### 4.3. Method of integration and the nonlinear fitting using origin

The Signal processing, Peak analysis and Fitting module in Origin is selected to process the measured current data. Using the FFT filter function in Signal Processing module to remove the electromagnetic interference of 50 Hz from the original current data shown in Supporting Fig. 1. As shown in Fig. 4a, the Actual Triboelectrification curve shows a very regular cycle, therefore we use the Integrate Peaks function in the Peak Analysis module to integrate the current curve. At the same time, the trend of negative charge conforms to the negative exponential curve, so we use the formula ExpAssoc in the Nonlinear Fitting function of Fitting module to fit the data of difference between positive and negative charges obtained by integration (Fig. 4b).

#### CRediT authorship contribution statement

All of authors (Xiuzhong Zhao, Xiao Lu, Qiwei Zheng, Lin Fang, Prof. Li Zheng, and Prof. Xiangyu Chen) declare no interest conflict on the paper entitled of "Study of contact electrification and electron transfer on dynamic liquid-liquid interface".

#### Declaration of Competing Interest

The authors declare that they have no known competing financial interests or personal relationships that could have appeared to influence the work reported in this paper.

#### Acknowledgements

This work was supported by the National Key R&D Project from Ministry of Science and Technology, China (2016YFA0202704), the National Natural Science Foundation of China (Grant No. 51775049), Science and Technology Commission of Shanghai Municipality (No.17020501000), the Program for Professor of Special Appointment (Eastern Scholar) at Shanghai Institutions of Higher Learning, the Ministry of Education of China (TP2017076), Science and Technology Commission of Shanghai Municipality (19DZ2271100), Beijing Natural Science Foundation (4192069), the Beijing Municipal Science and Technology Commission (Z171100000317001), Young Top-Notch Talents Program of Beijing Excellent Talents Funding (2017000021223ZK03), Beijing Nova Program (Z201100006820063) and Youth Innovation Promotion Association CAS (2021165).

#### Appendix A. Supporting information

Supplementary data associated with this article can be found in the online version at [doi:10.1016/j.nanoen.2021.106191](https://doi.org/10.1016/j.nanoen.2021.106191).

#### References

- [1] F.-R. Fan, Z.-Q. Tian, Z.L. Wang, Flexible triboelectric generator, *Nano Energy* 1 (2012) 328–334.
- [2] Z.L. Wang, L. Lin, J. Chen, S. Niu, Y. Zi. *Triboelectric Nanogenerators*, Springer, 2016.
- [3] Z.L. Wang, Triboelectric nanogenerator (TENG)—sparking an energy and sensor revolution, *Adv. Energy Mater.* 10 (2020), 2000137.
- [4] J. Shao, M. Willatzen, T. Jiang, W. Tang, X. Chen, J. Wang, Z.L. Wang, Quantifying the power output and structural figure-of-merits of triboelectric nanogenerators in a charging system starting from the Maxwell's displacement current, *Nano Energy* 59 (2019) 380–389.
- [5] Y. Chen, Y. Jie, N. Wang, Z.L. Wang, X. Cao, Novel wireless power transmission based on Maxwell displacement current, *Nano Energy* 76 (2020), 105051.
- [6] X. Ma, S. Li, S. Dong, J. Nie, M. Iwamoto, S. Lin, L. Zheng, X. Chen, Regulating the output performance of triboelectric nanogenerator by using P (VDF-TrFE) Langmuir monolayers, *Nano Energy* 66 (2019), 104090.
- [7] R. Lei, Y. Shi, Y. Ding, J. Nie, S. Li, F. Wang, H. Zhai, X. Chen, Z. Wang, Sustainable high voltage source based on triboelectric nanogenerator with charge accumulation strategy, *Energy Environ. Sci.* (2020).
- [8] L. Zheng, Y. Wu, X. Chen, A. Yu, L. Xu, Y. Liu, H. Li, Z.L. Wang, Self-powered electrostatic actuation systems for manipulating the movement of both microfluid and solid objects by using triboelectric nanogenerator, *Adv. Funct. Mater.* 27 (2017), 1606408.
- [9] J. Nie, Z. Ren, J. Shao, C. Deng, L. Xu, X. Chen, M. Li, Z.L. Wang, Self-powered microfluidic transport system based on triboelectric nanogenerator and electrowetting technique, *ACS Nano* 12 (2018) 1491–1499.
- [10] X. Peng, K. Dong, C. Ye, Y. Jiang, S. Zhai, R. Cheng, D. Liu, X. Gao, J. Wang, Z. L. Wang, A breathable, biodegradable, antibacterial, and self-powered electronic skin based on all-nanofiber triboelectric nanogenerators, *Sci. Adv.* 6 (2020) 9624.
- [11] W. Tang, B.D. Chen, Z.L. Wang, Recent progress in power generation from water/liquid droplet interaction with solid surfaces, *Adv. Funct. Mater.* 29 (2019), 1901069.
- [12] L. Xu, T. Jiang, P. Lin, J.J. Shao, C. He, W. Zhong, X.Y. Chen, Z.L. Wang, Coupled triboelectric nanogenerator networks for efficient water wave energy harvesting, *ACS Nano* 12 (2018) 1849–1858.
- [13] J. Nie, Z. Ren, L. Xu, S. Lin, F. Zhan, X. Chen, Z.L. Wang, Probing contact-electrification-induced electron and ion transfers at a liquid–solid interface, *Adv. Mater.* 32 (2020), 1905696.
- [14] J. Nie, Z. Wang, Z. Ren, S. Li, X. Chen, Z.L. Wang, Power generation from the interaction of a liquid droplet and a liquid membrane, *Nat. Commun.* 10 (2019) 1–10.
- [15] W. Xu, X. Zhou, C. Hao, H. Zheng, Y. Liu, X. Yan, Z. Yang, M. Leung, X.C. Zeng, R. X. Xu, SLIPS-TENG: robust triboelectric nanogenerator with optical and charge transparency using a slippery interface, *Natl. Sci. Rev.* 6 (2019) 540–550.
- [16] P. Jiang, L. Zhang, H. Guo, C. Chen, C. Wu, S. Zhang, Z.L. Wang, Signal output of triboelectric nanogenerator at oil–water–solid multiphase interfaces and its application for dual-signal chemical sensing, *Adv. Mater.* 31 (2019), 1902793.
- [17] L. Zheng, S. Dong, J. Nie, S. Li, Z. Ren, X. Ma, X. Chen, H. Li, Z.L. Wang, Dual-stimulus smart actuator and robot hand based on a vapor-responsive PDMS film and triboelectric nanogenerator, *ACS Appl. Mater. Interfaces* 11 (2019) 42504–42511.
- [18] L. Han, M. Peng, Z. Wen, Y. Liu, Y. Zhang, Q. Zhu, H. Lei, S. Liu, L. Zheng, X. Sun, Self-driven photodetection based on impedance matching effect between a triboelectric nanogenerator and a MoS<sub>2</sub> nanosheets photodetector, *Nano Energy* 59 (2019) 492–499.
- [19] Z. Wen, J. Fu, L. Han, Y. Liu, M. Peng, L. Zheng, Y. Zhu, X. Sun, Y. Zi, Toward self-powered photodetection enabled by triboelectric nanogenerators, *J. Mater. Chem. C* 6 (2018) 11893–11902.
- [20] W. Du, J. Nie, Z. Ren, T. Jiang, L. Xu, S. Dong, L. Zheng, X. Chen, H. Li, Inflammation-free and gas-permeable on-skin triboelectric nanogenerator using soluble nanofibers, *Nano Energy* 51 (2018) 260–269.
- [21] S. Li, Y. Fan, H. Chen, J. Nie, Y. Liang, X. Tao, J. Zhang, X. Chen, E. Fu, Z.L. Wang, Manipulating the triboelectric surface charge density of polymers by low-energy helium ion irradiation/implantation, *Energy Environ. Sci.* 13 (2020) 896–907.
- [22] S. Li, J. Nie, Y. Shi, X. Tao, F. Wang, J. Tian, S. Lin, X. Chen, Z.L. Wang, Contributions of different functional groups to contact electrification of polymers, *Adv. Mater.* 32 (2020), 2001307.
- [23] L.L. Sun, S.Q. Lin, W. Tang, X. Chen, Z.L. Wang, Effect of redox atmosphere on contact electrification of polymers, *ACS Nano* 14 (2020) 17354–17364.
- [24] C. Xu, Y. Zi, A.C. Wang, H. Zou, Y. Dai, X. He, P. Wang, Y.C. Wang, P. Feng, D. Li, On the electron-transfer mechanism in the contact-electrification effect, *Adv. Mater.* 30 (2018), 1706790.
- [25] S. Lin, L. Xu, A.C. Wang, Z.L. Wang, Quantifying electron-transfer in liquid-solid contact electrification and the formation of electric double-layer, *Nat. Commun.* 11 (2020) 1–8.
- [26] F. Zhan, A.C. Wang, L. Xu, S. Lin, J. Shao, X. Chen, Z.L. Wang, Electron transfer as a liquid droplet contacting a polymer surface, *ACS Nano* (2020).
- [27] Y.K. Liu, W.L. Liu, Z. Wang, W.C. He, Q. Tang, Y. Xi, X. Wang, H.Y. Guo, C.G. Hu, Quantifying contact status and the air-breakdown model of charge-excitation triboelectric nanogenerators to maximize charge density, *Nat. Commun.* 11 (2020) 1599.
- [28] W.C. He, W.L. Liu, J. Chen, Z. Wang, Y.K. Liu, X.J. Pu, H.M. Yang, Q. Tang, H. K. Yang, H.Y. Guo, C.G. Hu, Boosting output performance of sliding mode triboelectric nanogenerator by charge space-accumulation effect, *Nat. Commun.* 11 (2020) 4277.

- [29] J. Chen, H.Y. Guo, X.M. He, G.L. Liu, Y. Xi, H.F. Shi, C.G. Hu, Enhancing performance of triboelectric nanogenerator by filling high dielectric nanoparticles into sponge PDMS film, *ACS Appl. Mater. Interfaces* 8 (2016) 736–744.
- [30] H. Baytekin, A. Patashinski, M. Branicki, B. Baytekin, S. Soh, B.A. Grzybowski, The mosaic of surface charge in contact electrification, *Science* 333 (2011) 308–312.
- [31] K. Roger, B. Cabane, Why are hydrophobic/water interfaces negatively charge d? *Angew. Chem. Int. Ed.* 51 (2012) 5625–5628.
- [32] R. Vácha, S.W. Rick, P. Jungwirth, A.G. de Beer, H.B. de Aguiar, J.-S. Samson, S. Roke, The orientation and charge of water at the hydrophobic oil droplet–water interface, *J. Am. Chem. Soc.* 133 (2011) 10204–10210.
- [33] D. Oliver, J. Chung, Flow about a fluid sphere at low to moderate Reynolds numbers, *JFM* 177 (1987) 1–18.
- [34] D.M. Sagar, Colin D. Bain, Jan R.R. Verlet, Hydrated Electrons at the Water/Air Interface, *J. Am. Chem. Soc.* 132 (2010) 6917–6919.
- [35] E.J. Hart, J.J.J.o.t.A.C.S. Boag, Absorption spectrum of the hydrated electron in water and in aqueous solutions, 84 (1962), 4090–4095.



**Xiuzhong Zhao** received his B.S. degree in physics from University of Jinan in 2017, and he is currently pursuing a M.S. in Shanghai University of Electric Power. He is currently co-trained by XiangYu Chen Group of Nanoenergy and Nanosystems (BINN), Chinese Academy of Sciences (CAS). His research interests are focused on the mechanism of liquid-liquid triboelectric nanogenerator.



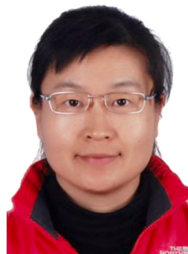
**Lu Xiao** received Bachelor degree in electrical engineering and automation from Lanzhou Jiaotong University. He is currently a master's degree student at Shanghai Electric Power University, majoring in renewable energy science and engineering. His current research interests focus on TENG-based sensors, self-powered nanosystems and TENG-based energy storage.



**Lin Fang** received his B.S. degree in electrical engineering and automation from Anhui Polytechnic University in 2019, and he is currently pursuing a M.S. in Shanghai University of Electric Power. His research interests are focused on TENG-based sensors, self-powered nanosystems.



**Qi Wei Zheng** received his B.S. degree in electrical engineering and automation from North China Electric Power University Science and Technology College in 2019, and he is currently pursuing a M.S. in Shanghai University of Electric Power. His research interests are focused on TENG-based energy storage and high voltage energy.



**Prof. Li Zheng** is a professor in Shanghai University of Electric Power. She received her M.S. from Chinese Academy of Sciences (CAS) in 2006 and Ph.D. degree from Shanghai Jiao Tong University in 2009. Her current research interests include nanowire lasers, nanostructure-based optoelectronic devices, nanogenerator, and self-powered nanosystems.



**Prof. Xiangyu Chen** received his B.S. degree in Electrical Engineering from Tsinghua University in 2007 and his Ph.D. in Electronics Physics from Tokyo Institute of Technology in 2013. Now he is a professor in Beijing Institute of nanoenergy and nanosystems, Chinese Academic of Sciences. His main research interests have been focused on the field of functional dielectric materials, self-powered nano energy system and the nonlinear optical laser system for characterizing the electrical properties of the devices.



**Prof. Zhong Lin (ZL) Wang** received his Ph.D. from Arizona State University in physics. He now is the Hightower Chair in Materials Science and Engineering, Regents' Professor, Engineering Distinguished Professor and Director, Center for Nanostructure Characterization, at Georgia Tech. Dr. Wang has made original and innovative contributions to the synthesis, discovery, characterization and understanding of fundamental physical properties of oxide nanobelts and nanowires, as well as applications of nanowires in energy sciences, electronics, optoelectronics and biological science. His discovery and breakthroughs in developing nanogenerators established the principle and technological road map for harvesting mechanical energy from environment and biological systems for powering a personal electronics. His research on self-powered nanosystems has inspired the worldwide effort in academia and industry for studying energy for micro-nano-systems, which is now a distinct disciplinary in energy research and future sensor networks. He coined and pioneered the field of piezotronics and piezophotonics by introducing piezoelectric potential gated charge transport process in fabricating new electronic and optoelectronic devices. Details can be found at: <http://www.nano-science.gatech.edu/>.